Abusive discharges to zero volt of VRLA/AGM monoblocs in 24V strings

H.Giess – B.Hughes
Accumulatoren-Fabrik Oerlikon
8050 Zürich Switzerland
e-mail: accu-info@accuoerlikon.com

Abstract Lead acid batteries may experience an abusive "deep" discharge condition when more than 100% of the nominal capacity is withdrawn. This paper describes the behavior of a VRLA/AGM battery under such discharge conditions by examining temperature and voltage parameters. As results show, certain designs of VRLA/AGM batteries exhibit a good tolerance against such abusive conditions.
A discharge for a period of 130h below 1.80Vpc did not induce, after recharge at the float voltage of 2.25Vpc, any capacity loss in such a battery.

I. Principal phenomena occurring during "deep" discharges of lead acid batteries

The term "deep" discharge of lead acid batteries is not unambiguously defined and the following meanings are used by the lead acid battery community:

a) Discharge of 80% of the rated C_8 to C_{10} capacity
b) Discharge of 100% of the rated C_8 to C_{10} capacity
c) Discharge below a final voltage of ~1.60Vpc
d) Discharge to a final voltage of ~ 0Vpc
e) Stand under load at ~0Vpc, for an extended time period

"Deep" discharges of the type a) and b) described above often result in capacity losses and active material shedding. These types of "deep" discharges were particularly troublesome for early antimony-free lead acid battery designs. The importance of the interface between the grid and the active material was recognized in the late 70's by researchers at Battelle Switzerland [1].
This premature capacity loss was dubbed "*PCL*" in the early 90's by Rand et al. [2] at CSIRO Australia. It involved the undesirable degradation of the positive active mass (PbO_2) in the vicinity of the grid. The addition of phosphoric acid to the electrolyte or more adequate manufacturing processes overcame this phenomenon.
Type c) "deep" discharges can induce, in batteries made from low antimony (Sb<1%), pure lead and binary lead calcium grid alloys a positive plate passivation phenomenon. This results in an extremely poor acceptance of charging current by the discharged battery under constant voltage recharge or in an extremely high (3Vpc) voltage during constant current charging. The inability of batteries made with above grid alloys to accept current during charging but still indicating "fully charged" voltage and current readings, caused many unpleasant surprises to their users. The passivation phenomenon was traced to the formation of a layer of insulating lead oxide (PbO) on the positive grid surface. The theoretical explanation for its formation was given by Ruetschi [3]. The PbO formed in an alkaline environment developing underneath a lead sulfate film as a result of a "deep" discharge. The basic technological fix for this passivation was outlined in the US Patent 4,092,462 (1978) and detailed in 1984 by Giess [4]. It involves the addition of at least 0.6% of tin to such alloys to prevent PbO formation.

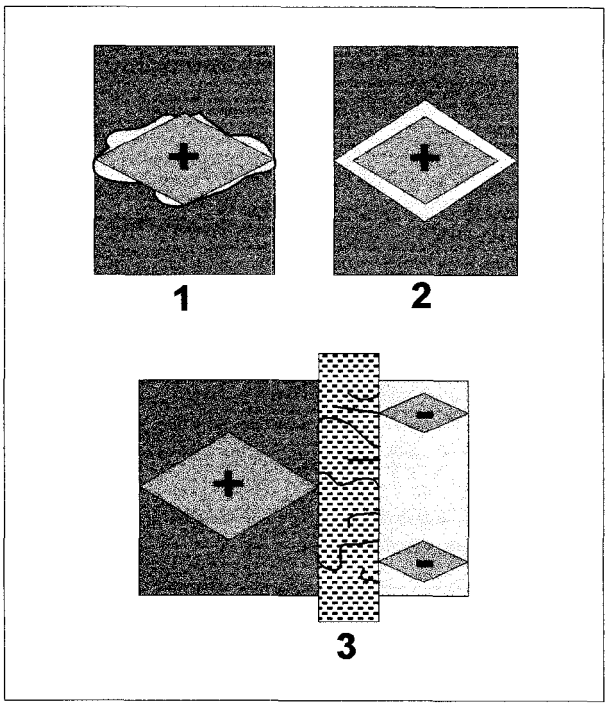

Fig 1. Schematic view of "deep" discharge damage modes 1) PCL – 2) PbO barrier – 3) Pb dendrites

The "deep" discharge types d) and e), which represent the most severe operating conditions, result, if not corrected, in all of above damage modes.

0-7803-3996-7/97/$10.00©1997 IEEE

Further damage in the form of internal lead dendrite shorts may also occur due to this extreme discharging.
The formation of lead dendrites is due to a mayor increase of lead sulfate solubility in the extremely dilute electrolyte, which is present at the end of a "deep" discharge. Under these conditions an acicular growth of minute lead crystals or dendrites develops on the negative plate, which penetrates through the separator to the positive plate. The individual plates of opposite polarity are thus shorted and parasitic internal discharge or bypassing of the charging current along electronic conducting paths takes place.

One of the technological fixes for this growth is the addition of an alkaline or alkaline earth sulfate salt to the sulfuric acid in order to suppress the lead sulfate solubility. Salt is added in such a quantity so as to maintain an ionic concentration of approximately 0.1mol [SO_4^-] ions also at the exhaustion point of all sulfuric acid resulting from the "deep" discharge.
The sulfate salt however may cause a more aggressive and corrosive environment at the negative strap resulting in premature failures, if not counteracted by appropriate alloy and manufacturing choices [5].
All the above described "deep" discharge difficulties can be observed in both flooded and electrolyte-starved battery designs although to varying degree of frequency and intensity.
With the introduction of electrolyte-starved VRLA batteries in both AGM and GEL designs and their use in unsupervised conditions, damage by "deep" discharge of the type d) and e) is not uncommon.
The purpose of this presentation is to show the evolution of voltage and temperature parameters of a 24V VRLA battery string under d) and e) "deep" discharge conditions.

2. Experimental

The zero volt discharge test was carried out with a 24V string of 6V100Ah (C_{10})VRLA/AGM monoblocs. To simulate the eventual effects of a compact assembly, the monoblocs were installed close together and lying flat, with the plates horizontally oriented. The monoblocs were spaced 10mm apart and partially encased in foam plastic. The discharge/charge sequence was carried out at a room temperature between 18 and 25°C with a natural, vertical air flow of ~0.06m.s^{-1}. Discharges were carried out with a constant resistive load of 2.14 Ohm giving a nominal current of 11.1A at 24V. The load resistor was connected during the entire discharge and 0 Volt phase of the battery string.
Battery charge was carried out with a regulated cc-cv/IU power supply with a 10A charging current and 2.25Vpc maximum voltage. No boost voltage was used during charge. The temperature of the monoblocs was monitored with type J thermocouples in direct contact with the case and with a Nippon Avionics TVS2000 thermal imaging system. This system can resolve 0.05°C temperature differences and can store images for further analysis with dedicated software [6]. The internal resistance of the string was followed with a Hioki 3550 (AC) Milliohmmeter.

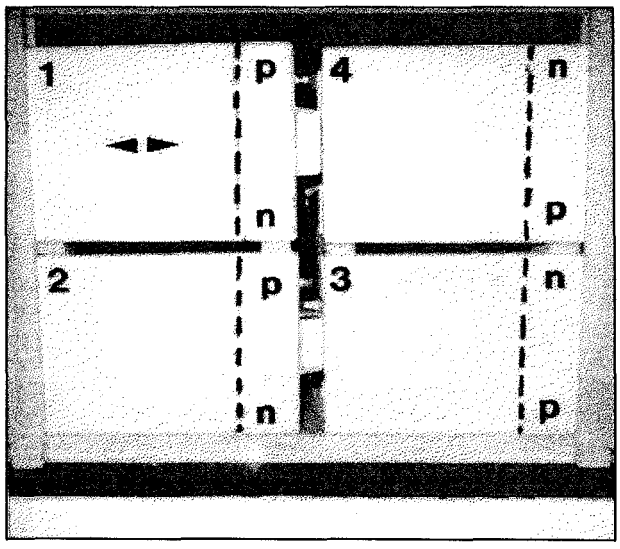

Fig 2. View of the 24V 100Ah string with monoblocs #1, 2, 3 and 4 in horizontal position during testing. P, n shows terminals and dotted line delimits the headspace.

3. Results

Electrical and capacity data
The usable capacity of a lead acid battery is limited generally by the amount of positive active material present and is given theoretically by the formula 0.224Ah.g^{-1} PbO_2. However, less than 50% of this capacity can be extracted at discharge rates above the 10 hour rate.
Additional capacity can only be extracted at very low current and voltage levels due to polarization, mass transfer limitations and internal resistance increases.

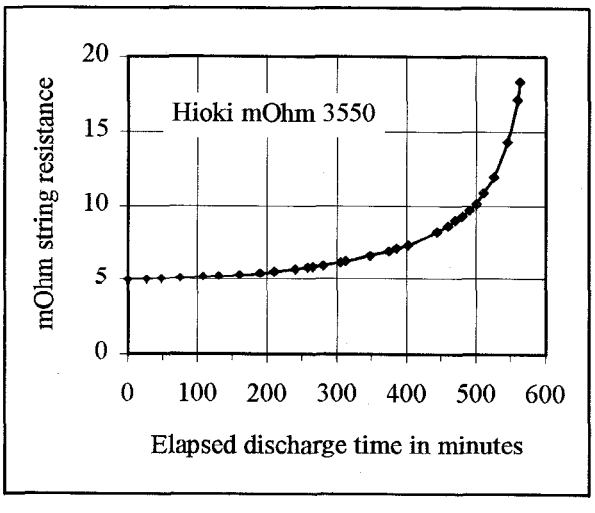

Fig 3. Evolution of the apparent internal resistance of the 24V/100Ah string during discharge to 1.80Vpc.

During a C_{10} discharge of a lead acid battery, the on-load voltage drops slowly but continuously from approximately 2.05Vpc to the final discharge voltage of 1.80Vpc. Beyond this point, the voltage decay accelerates due to a steep rise in internal resistance (see Fig 7) caused by a depletion of ionic species [SO_4^-] and the formation of water.

With very deep battery discharge certain cells or monoblocs can be driven into reverse i.e. show a negative voltage (see Fig 4). This reversal results in additional heat and possibly also gas generation.

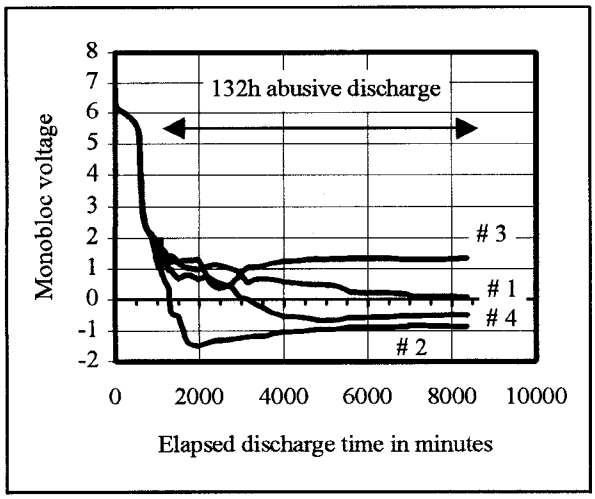

Fig 4. Evolution of the monobloc voltage during the regular and "deep" discharge (monobloc #1, 2, 3 and 4). Note polarity reversal of # 2 and 4 after ~1000 and ~3000 minutes respectively of discharge.

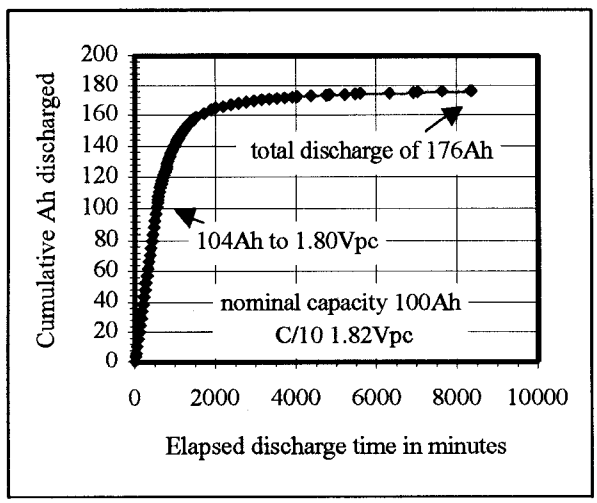

Fig 5. Cumulative ampere hours extracted during the full discharge period i.e. 176% of the nominal capacity.

The total amount of ampere hours extracted from the 24V string of nominal 100Ah capacity, amounted to 176Ah as shown in Fig 5. However, only 104Ah were discharged at or above the I_{10} current.

Lead acid batteries display a heat pump behavior i.e. they cool down during capacity withdrawal. However, this behavior is noticeable only at very low discharge rates when the Joule heating is not over-compensating the cool-down effect.
Heat evolution is proportional to the internal resistance and polarization or in other words the difference between open circuit voltage and on-load voltage.
The temperature, as measured on the surface of the ABS monobloc case is shown in Fig 6.

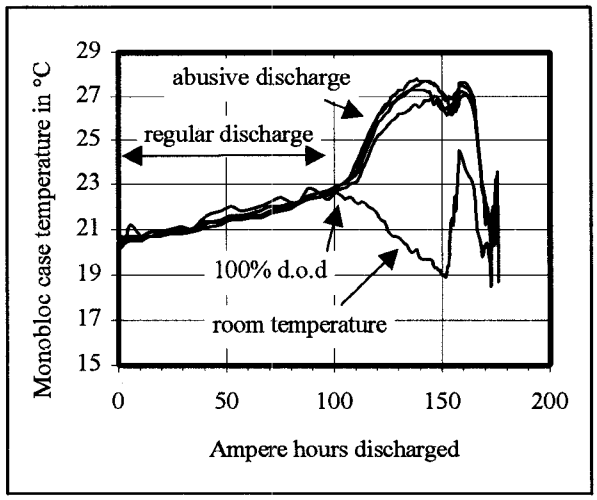

Fig 6. Evolution of the monobloc case and ambient air temperature during the regular and "deep" discharge phase. Note the quick temperature rise beyond the 100% depth or 100Ah of discharge.

The internal resistance of the battery string was followed through the complete "deep" or abusive discharge period and a twenty-fold increase to 350mOhm was observed.

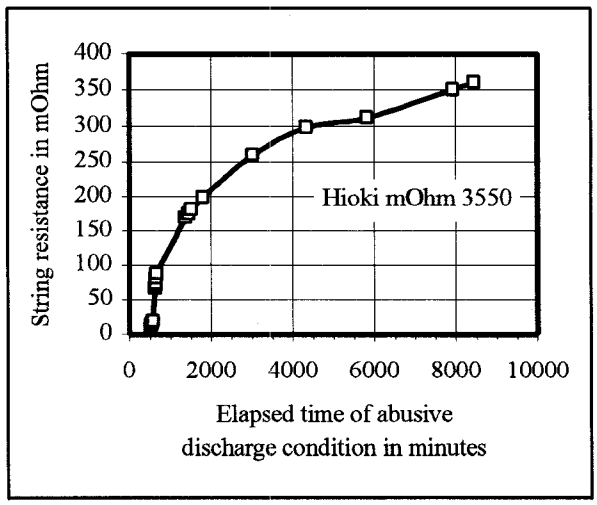

Fig 7. Evolution of the internal resistance of the 24V string during the "deep" discharge beyond 1.80Vpc.

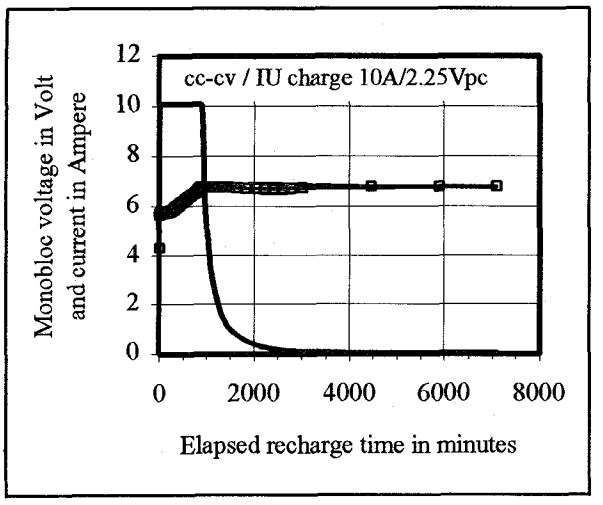

Fig 8. Evolution of the monobloc voltages and charging current during recharge from "zero" volt after the abusive "deep" discharge.

The string was recharged under cc-cv/IU conditions without a boost voltage phase. As can be seen in Fig 8, no sign of excessive polarization was noticeable in the voltage vs. time trace. The battery string accepted the I_{10} charge current of 10A with an initial cell voltage of only ~1.4Vpc.

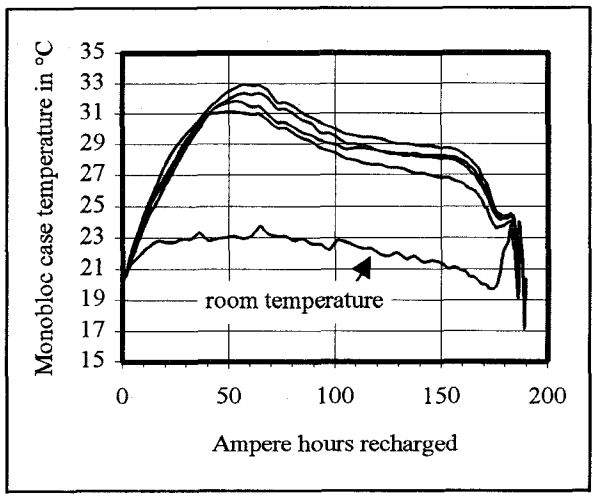

Fig 9. Evolution of the monobloc case and ambient temperature during the cc-cv/IU recharge from "zero" volt.

During the recharge of the battery a linear rise of the temperature was noted peaking at 33°C case temperature after approximately 50Ah or 30% recharge.
The recharge continued under $I_{constant}$ conditions for about 15 hour or to ~80% recharge in terms of the previous extracted 176Ah. This quick recharge is related to the very low internal resistance and the absence of PbO barriers on the positive VHT grid alloy.

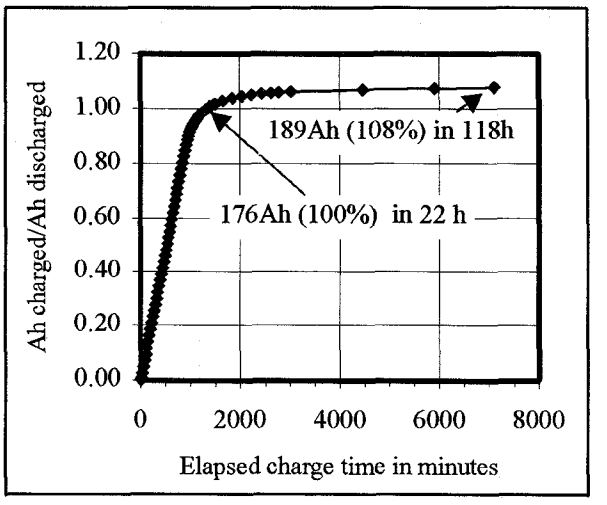

Fig 10. Cumulative ampere hours recharged under cc-cv/IU 10A/2.25Vpc conditions

In addition to the evaluation of the thermal behavior of the 24V string during the "deep" discharge sequence, data was also collected on the available capacity after 120h of charge so as to evaluate the ability of the battery to cope with a renewed power outage. The string was again discharged at 20°C using the 2.14 Ohm resistor and the time taken to reach 21.6V was measured.
During this discharge the "coup de fouet" voltage transient was well pronounced, indicating the absence of significant amounts of residual sulfate. Also, no notable spread of the individual monobloc discharge voltages was observed.

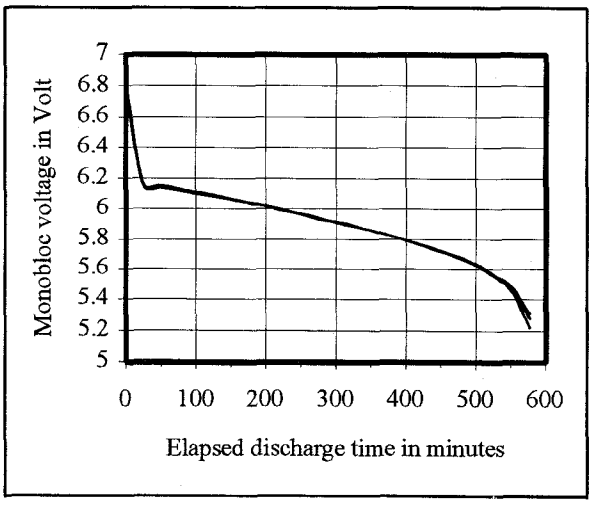

Fig 11. Evolution of monobloc voltages during the capacity discharge following the abusive "deep" discharge sequence.

As shown in table 1, a capacity of 102% of that originally found before the "deep" discharge sequence was measured after the 0 Volt test. This indicates that the selected VRLA/AGM design can tolerate at least one abusive "deep" discharge without permanent damage.

Discharge test	Ampere hours (integrated)	Time to 1.80Vpc	Capacity in percent
Before 0V test	103.9	9:10	100
After 0V test	108.8	9:23	102

Table 1. Summary of the string capacity before and after the abusive zero volt "deep" discharge.

Thermal imaging of the monoblocs

The imaging of the monoblocs in emitted infrared radiation is a convenient method of determining the site and extend of localized heat evolution. Due to >95% transparency of the ABS case in an IR wavelength of 3-5µm, used for the analysis, not only the surface temperature of the ABS cell cases but also the temperature of the components in the cell interior could be measured with good lateral definition.

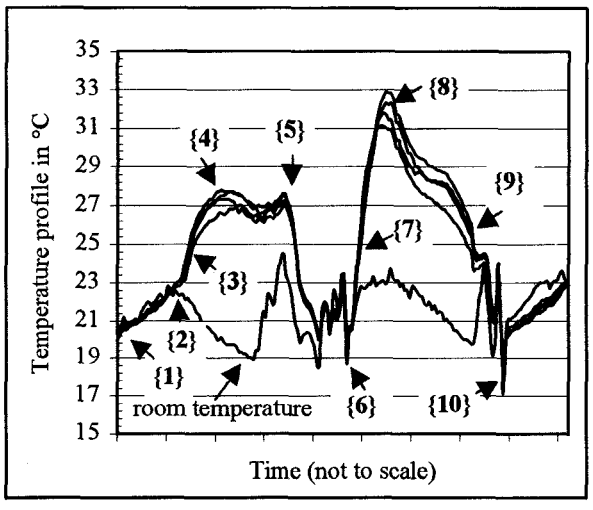

Fig 12. Temperature vs. time profile covering the first capacity discharge, the abusive discharge, the recharge and the second capacity discharge . The numbers in bracket {x} refer to selected points in time at which thermal images were taken. These images are shown in the following figures.

During the entire experimental run, the TVS2000 camera was pointed at the 24V monobloc string and thermal images were recorded every 24 to 48 minutes from the same position and angle. The temperature range and sensitivity of the TVS2000 was adapted automatically so as to encompass the minimum and maximum temperature of the observed area. The images were then processed with the PicEd™ software. In the following sequence of images the typical temperature distribution is shown in relation to events during the discharge-charge-discharge sequence at time points numbered {1} to {10} in Fig 12. The first image (Fig 13) represents the string under float charge with a temperature of 20.0 to 20.5°C. The position of the plate groups in the monoblocs can be detected through small temperature differences between the "cool" plates and the "warm" cell head space (+0.2°C). The second image (Fig 14) shows the temperature distribution at the end of the 11A discharge to 1.80Vpc with very little discharge induced temperature rise.

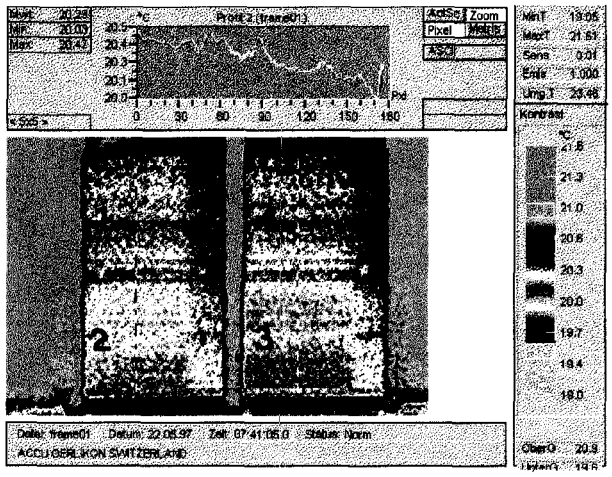

Fig 13. Thermal image of the string during 2.25Vpc float charge at time point {1} just before the discharge and at a temperature of 20.0 to 20.5°C

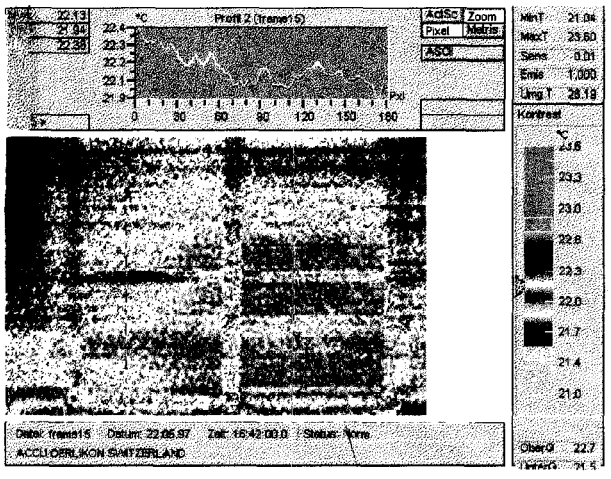

Fig 14. Thermal image of the string at time point {2} at end of the first 11A discharge to 1.80Vpc. Only a room temperature induced rise is noted with a temperature of 22.0-22.4°C.

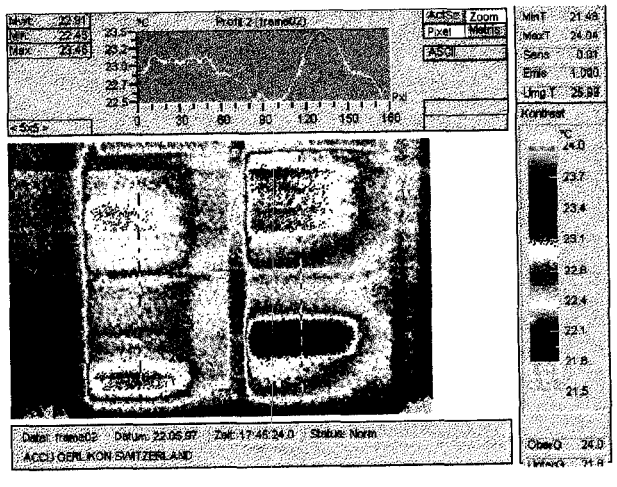

Fig 15. Thermal image at time point {3} after 1h of additional discharge beyond 1.80Vpc and monobloc voltages of 5.23, 5.20, 4.87 and 5.06V. Note the "hot" cell in monobloc #3.

Fig 15 shows that as the discharge proceeds beyond 1.80Vpc or time point {3}, the center cell of monobloc #3 generates heat and the temperature rises locally to approximately 23.7°C in comparison to a temperature average of 22.5°C. Monoblocs #3 also shows a voltage of 4.87Vpc compared with 5.06 to 5.23V for the rest of the monoblocs.

During the abusive "deep" discharge period, the maximum monobloc temperature is reached after withdrawing approximately 140% of the rated capacity (100Ah) or in other words 7h additional discharge time down to monobloc voltages of 2.01, 1.67, 1.67, 1.94V respectively. The case temperatures reached 26.6 to 27.8°C and a discharge current of 3.6A was flowing.
As can be seen from Fig 16, mainly center cell temperature distribution effects are noticeable.

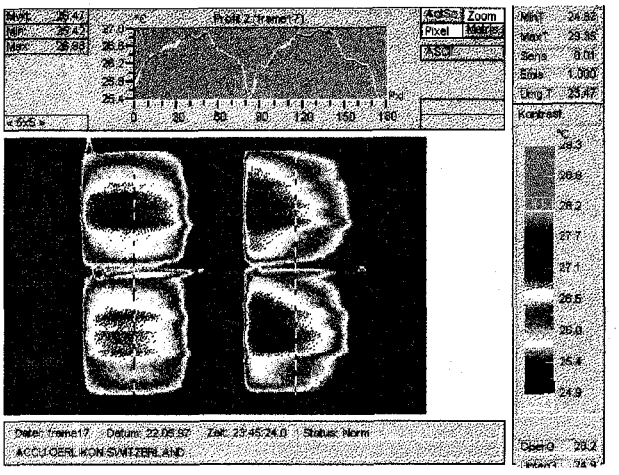

Fig 16. Thermal image at time point {4} showing the peak heat generation point during the abusive "deep" discharge. Monobloc voltages were at 1.67 to 2.01V with 3.5A current flow and a monobloc temperature of 26.6 to 27.8°C.

After approximately 17h of discharge below 1.80Vpc, at time point {5} and, a total of 160Ah withdrawn, the monobloc # 2 shows a polarity reversal to –0.47V with the remainder of the units at +1.36, +1.23 and +0.82V respectively. A current of 1.4A was flowing at this point. The monobloc with the reversed polarity (#2), shown in Fig 17, has a significantly hotter center cell temperature of approximately 27.7°C denoting the probable location of the reversed cell.
At the completion of the 132h of discharge beyond 1.80Vpc, the under-load-voltage of the monoblocs stabilized at +0.10V, -0.87V, +1.35V and -0.52V, with current of 0.03A flowing. The monoblocs had now cooled down to a temperature of 20 to 21°C.
The thermal image at time point {6} at the end of the abusive discharge "deep" phase, is shown in Fig 18. No major thermal irregularities are noticeable at this stage.
Following the abusive "deep" discharge phase the string was recharged under cc-cv/IU conditions of 10A and 2.25Vpc or 27V.

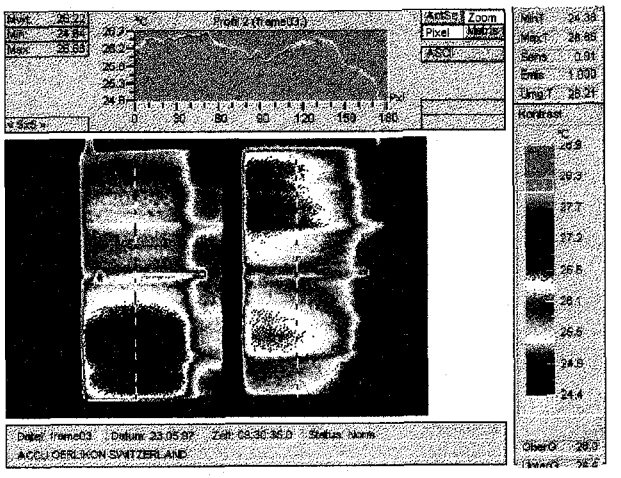

Fig 17. Thermal image at time point {5} and with 160Ah discharged. Monobloc #2 is in polarity reversal (-0.47V) and the middle cell showing a significantly hotter temperature of 27.7°C.

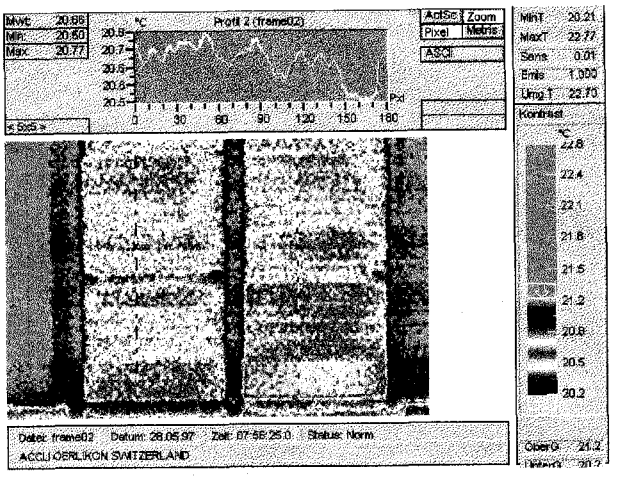

Fig 18. Thermal image at time point {6} and at the end of the abusive "deep" discharge phase with monobloc #2 and 4 in polarity reversal.

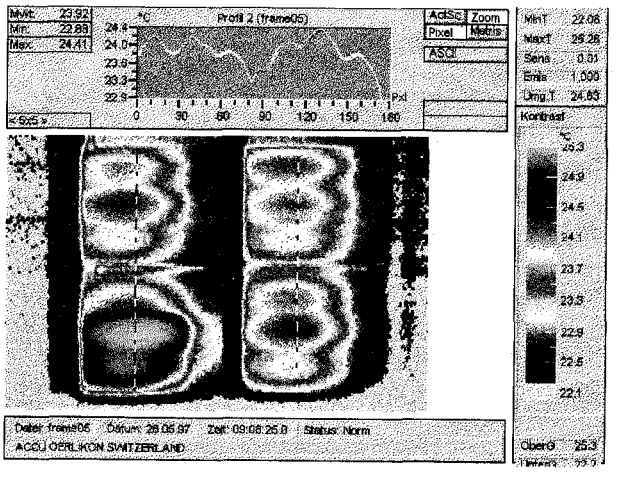

Fig 19. Thermal image at time point {7} with 72 minutes of charge at 10A and monobloc voltages at 5.70 to 5.75V. Note the well developed heating of the cells of monobloc #2 having shown voltage reversal and localized heat generation during the "deep" discharge phase.

During the charge phase a maximum temperature of 31 to 33°C was reached after approximately 50Ah or 30% recharge with the monoblocs showing a voltage of 5.85 to 5.87V at a charging current of 10A.
The temperature was quite uniform throughout the cells of each monobloc and between the monoblocs except for the middle cell of #4. Here a temperature of 32°C was found at the bottom of the plate group.

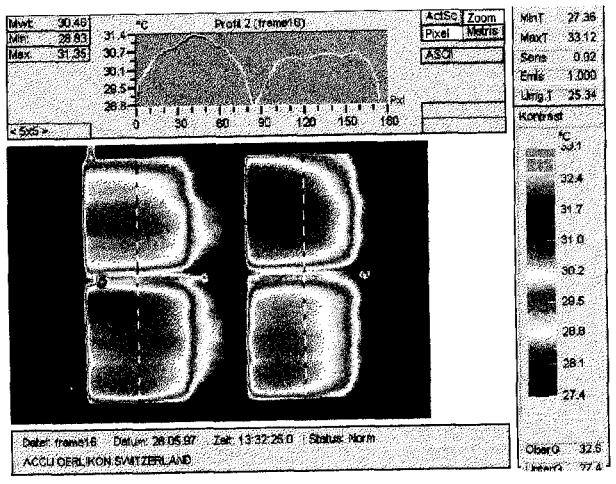

Fig 20. Thermal image at peak heat generation during the recharge phase at time point **{8}** with 5.8V and 10A charging current.

This is a critical period during recharge when the full charging current is flowing and the cells are polarized to less than 2Vpc. If the thermal energy transfer to the surrounding environment is impeded, a continuous steady rise in monobloc temperature may set in, which can result in a so called "thermal runaway". The proper design of a battery cabinet has to take account of such conditions if a low voltage disconnect of all the electrical loads cannot be assured.
Heat is generated up to ~90% of the recharge (160Ah) or for ~21h from the start of the recharge. The thermal image, at ~100% recharge, at time point **{9}**, is shown in Fig 21.

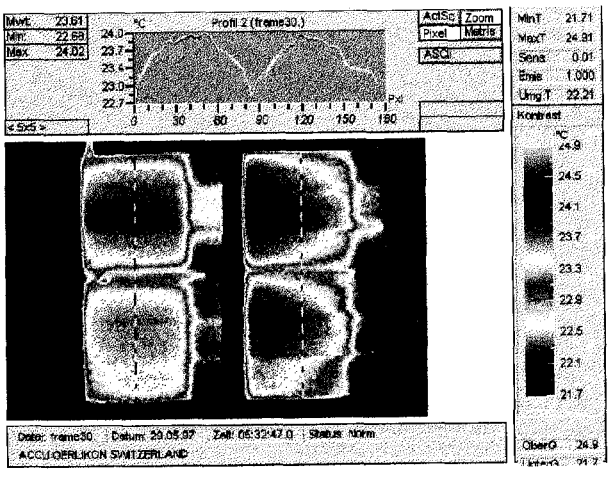

Fig 21. Thermal image at time point **{9}** or 100% recharge.

The final thermal image (Fig 22) was taken at the conclusion of the ~120h charge period with the monobloc temperature now back at room temperature (20°C) and the float current having decayed to 25mA. The current shows no noise component and its value was slightly lower than that found under identical conditions before the abusive discharge sequence. This would indicate an absence of micro-shorts between plates. The monobloc voltages were close together at 6.74, 6.74, 6.79 and 6.76V respectively.

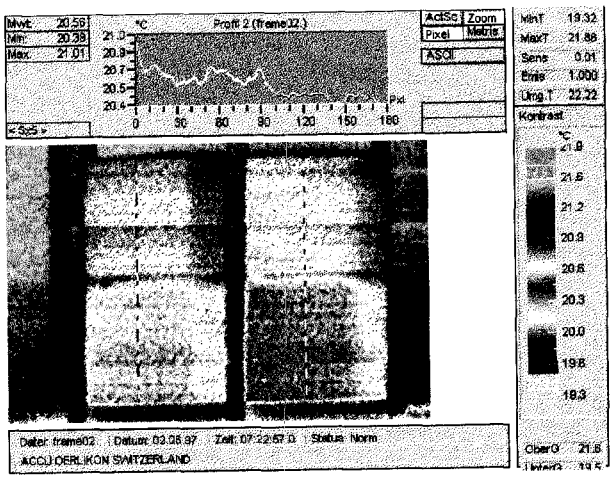

Fig 22. Thermal image at time point **{10}** at the end of the 120h recharge under float voltage condition of 2.25Vpc.

3. Conclusion

The "deep" discharge of lead acid batteries, resulting in the withdrawal of significantly more than 100% of the nominal capacity, causes a high level of heat generation. In the tested 6V100Ah monoblocs heat was generated which elevated the temperature to 28°C during discharge and 33° during recharge resulting in an 8 respectively 13°C rise above room temperature. This thermal effect has to be taken into account in the design of thermally safe battery installations.

With the appropriate battery design choices such as a minimum quantity of tin in the positive grid alloy and a lead sulfate solubility suppressant in the electrolyte, extremely abusive "deep" discharges lasting up to 130h (5 days) and withdrawing 170% of the nominal C/10 capacity can be tolerated. The tested VRLA/AGM battery string did not suffer, in terms of capacity loss, from such a discharge.

Whereas an abusive "deep" discharge can be tolerated on an emergency basis in battery installations, this operational mode should not be implemented as the normal mode since the operational robustness of the installation may be reduced.

References

[1] H.Giess et al. Battelle unpublished research reports 1973-1978
[2] D.Rand et al. in Proceedings of the 2nd meeting of the ALBAC PCL study group September 1994
[3] P.Ruetschi J.Electrochem. Soc. 120, 331 (1973)
[4] H.Giess in Proceedings of the 166th society meeting of The Electrochemical Society, New Orleans, 1984
[5] Pavlov et al. J.Electrochem. Soc. 142, 2919 (1995)
[6] H.Giess in Proceedings of the 5ELBC, Barcelona, 1995, to be published in the Journal of Power Sources 1997